DI-MESON LIFETIME MEASUREMENT WITH DIRAC

B. Adeva[o], L. Afanasyev[l], M. Benayoun[d], Z. Berka[b], A. Benelli[p], V. Brekhovskikh[n], G. Caragheorgheopol[m], T. Cechak[b], M. Chiba[j], S. Constantini[p], S. Constantinescu[m], A. Doudarev[l], D. Drijard[a], I. Evangelou[s], M. Ferro-Luzzi[a], M.V. Gallas Torreira[a,o], J. Gerndt[b], R. Giacomich[f], P. Gianotti[e], D. Goldin[p], F. Gomez[o], A. Gorin[n], O. Gortchakov[l], C. Guaraldo[e], M. Hansroul[a], R. Hosek[b], M. Iliescu[e,m], M. Jabitski[l], N. Kalinina[r], V. Karpoukhine[l], J. Kluson[b], M. Kobayashi[g], P. Kokkas[s], V. Komarov[l], A. Koulikov[l], A. Kouptsov[l], V. Krouglov[l], L. Krouglova[l], K.-I. Kuroda[k], A. Lamberto[f], A. Lanaro[a], V. Lapshin[n], R. Lednicky[c], P. Leruste[d], P. Levi Sandri[e], A. Lopez Aguera[o], V. Lucherini[e], T. Maki[i], I. Manuilov[n], N. Manthos[s], L. Montanet[a], J.-L. Narjoux[d], L. Nemenov[a,l], M. Nikitin[l], T. Nunez Pardo[o], K. Okada[h], V. Olchevskii[l], M. Pentia[m], A. Penzo[f], J.-M. Perreau[a], C. Petrascu[e,m], M. Plo[o], T. Ponta[m], D. Pop[m], G.F. Rappazzo[f], A. Riazantsev[n], J.M. Rodriguez[o], A. Rodriguez Fernandez[o], V. Rykalin[n], C. Santamarina[p], J. Saborido[o], J. Schacher[q], C. Schuetz[p], A. Sidorov[n], J. Smolik[c], F. Takeutchi[h], A. Tarasov[l], L. Tauscher[p], M.J. Tobar[o], F. Triantis[s], S. Trousov[r], P. Vazquez[o], S. Vlachos[p], V. Yazkov[r], Y. Yoshimura[g], P. Zrelov[l]

[a] CERN, Geneva, Switzerland
[b] Czech Technical University, Prague, Czech Republic
[c] Institute of Physics ASCR, Prague, Czech Republic
[d] LPNHE des Universites Paris VI/VII, IN2P3-CNRS, France
[e] INFN - Laboratori Nazionali di Frascati, Frascati, Italy
[f] Trieste University and INFN-Trieste, Italy
[g] KEK, Tsukuba, Japan. [h] Kyoto Sangyou University, Japan
[i] UOEH-Kyushu, Japan. [j] Tokyo Metropolitan University, Japan
[k] Waseda University, Japan. [l] JINR Dubna, Russia
[m] National Inst. for Physics and Nucl. Engin. IFIN-HH, Bucharest, Romania
[n] IHEP Protvino, Russia. [o] Santiago de Compostela University, Spain
[p] Basel University, Switzerland. [q] Bern University, Switzerland
[r] Skobeltsyn Institute for Nuclear Physics of Moscow State University
[s] University of Ioannina, Greece

The main goal of the DIRAC experiment is to measure the $\pi^+\pi^-$ atom lifetime of about 3 fs with a precision of 10%. This measurement provides, in a model-independent way, the difference between the isoscalar and isotensor strong S–wave $\pi\pi$ scattering lengths, $|a_0 - a_2|$. Pion–pion scattering lengths have been calculated in the framework of Chiral Perturbation Theory with an accuracy better than 3%, therefore such a measurement will be a sensitive check of the understanding of chiral symmetry breaking in QCD and effective theories at low energies. After a brief introduction, we will describe in this paper the DIRAC experiment and measurement method, together with the preliminary results of the analysis of the data taken in 1999, 2000 and 2001.

PACS numbers: 24.85+p

1. Introduction.

At present, low energy pion–pion scattering cannot be calculated directly in QCD. However, the approach based on an effective Lagrangian and Chiral Perturbation Theory (χPt) [1] can be used to calculate the strong S–wave $\pi\pi$ scattering lengths with an accuracy better than 3% [2]. These predictions have not been yet tested with such accuracy and new experimental efforts are thus desirable. The results of χPt have been obtained assuming that the value of the quark condensate is large, as it was confirmed by the recent analysis of $\pi\pi$ scattering phases [3]. There is an alternative scenario which allows an arbitrary value of the quark condensate [4]; if this is large, the $\pi\pi$ scattering lengths of [4] must coincide with those of [2]. But if the quark condensate is small, then the scattering lengths may be greater than the predicted values in χPt.

Dimeson atoms like the $A_{2\pi}$, which is a $\pi^+\pi^-$ Coulomb bound state, are an ideal place to study low energy QCD processes. In particular, there is a precise relation between the $A_{2\pi}$ lifetime and the strong S–wave pion–pion scattering lengths. By measuring this lifetime [5] it is thus possible to perform a crucial test of our understanding of chiral symmetry breaking in QCD and draw some conclusions about the magnitude of the quark condensation. $A_{2\pi}$ atoms were already observed for the first time in an experiment carried out at the Serpukov proton synchrotron [6].

The $A_{2\pi}$ decays mainly by strong interaction into $\pi^0\pi^0$. $\Gamma = \tau^{-1} = \Gamma_{2\pi_0} + \Gamma_{2\gamma}$, $\Gamma_{2\gamma}/\Gamma_{2\pi_0} \sim 4 \times 10^{-3}$. Its Bohr radius is about 387 fm, the Bohr momentum is 0.5 MeV/c, its binding energy is 1.858 keV, and $J^{PC} = 0^{++}$. Recent calculations [7, 8, 9] at NLO in isospin symmetry breaking show the following relation [9] between the $\Gamma_{2\pi_0}$ and S–wave $\pi\pi$ scattering lengths:

$$\Gamma_{2\pi_0}^{NLO} = \frac{2}{9}\alpha^3 p^* (a_0 - a_2 + \varepsilon)^2 (1 + K) \tag{1.1}$$

$$p^* = \sqrt{M_{\pi^+}^2 - M_{\pi^0}^2 - \frac{1}{4}\alpha^2 M_{\pi^+}^2} \tag{1.2}$$

Where a_0 and a_2 are the $\pi\pi$ scattering lengths for isospin $I = 0$ and $I = 2$, α is the fine structure constant, $\varepsilon = (0.58 \pm 0.16) \times 10^{-2}$ is the isospin breaking effect contribution [15], and $K = 1.07 \times 10^{-2}$ takes into account electromagnetic corrections. By measuring the lifetime of the $A_{2\pi}$ with a precision of $\delta\tau/\tau \sim 10\%$, we can get a prediction for the difference $\Delta = |a_0 - a_2|$ with a precision of $\delta\Delta/\Delta \sim 5\%$. It is the primary goal of the DIRAC experiment [16] to measure τ for the $A_{2\pi}$ with a precision of 10%.

2. Pionium production and detection.

2.1. Pionium production.

The DIRAC/PS212 experiment operates at the T8 beam line of the CERN Proton Synchrotron accelerator. 24 GeV/c protons (10^{11} per spill) are made to collide with a fixed target of suitable thickness and atomic number, Z. The $A_{2\pi}$ atoms originate from Coulomb final state interactions of pion pairs coming from the target fragmentation and short–lived sources decays (ρ, ω, K*, ...), but not from long–lived sources (η, η', K_s^0, ...). The differential cross–section for the $A_{2\pi}$ production is proportional to the double inclusive production cross–section of $\pi^+\pi^-$ pairs from short lived sources without taking into account the Coulomb interaction between them [5]:

$$\frac{d\sigma_n^A}{d\vec{p}_A} = (2\pi)^3 \frac{E_A}{M_A} |\Psi_n(0)|^2 \left(\frac{d\sigma_s^0}{d\vec{p}_1 d\vec{p}_2} \right)_{\vec{p}_1=\vec{p}_2=\vec{p}_A/2} \tag{2.1}$$

where $\vec{p}_A$, E_A and M_A are the momentum, energy and mass of the $A_{2\pi}$ atom in the laboratory system. $\Psi_n(0)$ is the hydrogen–like atomic wave function at the origin, with principal quantum number n.

2.2. Pionium detection.

In vacuum, $A_{2\pi}$ atoms would quickly go to $\pi^0\pi^0$, but inside the production target they interact with the surrounding atoms and may break up (ionize) into a $\pi^+\pi^-$ pair with very small relative momentum in the center of mass frame ($Q < 3$ MeV/c) and a small opening angle in the laboratory frame ($\theta < 3$ mrad). These $\pi^+\pi^-$ atomic pairs are the signal DIRAC is searching for. The $A_{2\pi}$ ionization as it travels through the target is a process that competes with the annihilation into $\pi^0\pi^0$. Our experimental method of lifetime measurement needs both processes to occur with similar probability. This can be achieved selecting a high-Z and thing target, for example:

target	Z	L(μm)	P$_{\rm dsc}$	P$_{\rm ann}$	P$_{\rm br}$
Ti	22	251	0.052	0.634	0.313
Ni	28	94	0.096	0.453	0.450
Pt	78	28	0.125	0.163	0.711

Here $P_{\rm br}$ is the atom breakup probability, $P_{\rm ann}$ is the annihilation probability, and $P_{\rm dsc}$ is the probability that the atoms leave the target in a discrete state and then annihilates in the vacuum tank where the target is located. The relation $P_{\rm br} + P_{\rm ann} + P_{\rm dsc} = 1$ is obviously satisfied. Looking at these probabilities in the table, it is clear that the most suitable target to measure the $A_{2\pi}$ lifetime is the Nickel one. On the other side, corrections to the Born single photon exchange approximation for the treatment of $A_{2\pi}$–target interactions are larger for Pt (1%) than there are for Ni (1%). The $A_{2\pi}$ breakup probability depends only on the atomic number of the target (Z), its length (L), the atom momentum ($p_{A_{2\pi}}$), and its lifetime (τ):

$$P_{\rm br} = 1 - P_{\rm dsc} - P_{\rm ann} = f(Z, L, p_{A_{2\pi}}, \tau) \tag{2.2}$$

The theoretical calculation of the previous function with a relative error of less than 1% is possible [10, 11, 12, 13] because we have a detailed knowledge of the cross–sections involved in the process, which is only a pure electromagnetic one.

On the other side, the breakup probability can be measured experimentally as the ratio of the atomic pairs detected over the number of produced atoms: $P_{\rm br} = n_A/N_A$. By comparing the experimental measurement with the theoretical prediction for a given target we can determine the $A_{2\pi}$ lifetime.

3. The DIRAC experimental apparatus.

The goal of detecting low relative momentum $\pi^+\pi^-$ pairs with a very small opening angle in the lab frame drives the DIRAC spectrometer design. A double arm spectrometer (see figure 1) able to deliver a resolution better than 1 MeV/c in the measurement of very low relative momentum particle pairs was commissioned in the 1998 autumn at the T8 beam line of the CERN PS. After the dipole magnet, the two spectrometer arms are inclined 5.7° degrees in the vertical direction with respect to the incoming proton beam. The channel aperture is about 1.2 msr. The target system permits an easy exchange of the target material (Ni, Pt, ...) if desired. Before the magnet we have the following detectors:

- Four planes of Microstrip Gas Chambers (MSGC) with GEM (Gas Electron Multiplier), to provide a measurement of pion tracks with a resolution of about 40 μm.

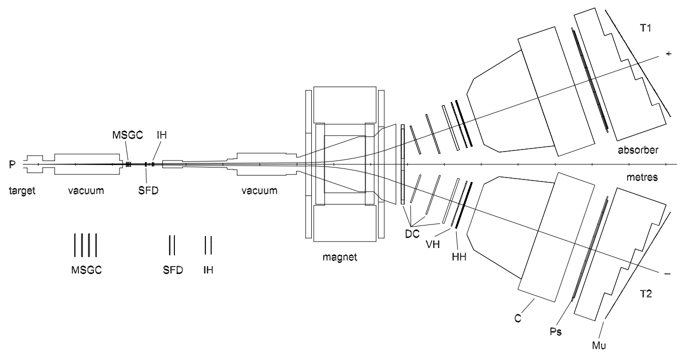

Fig. 1. The double–arm spectrometer of the DIRAC setup.

- A Scintillating Fiber Detector (SFD) made up of three layers which contributes to the particle tracking and also to the trigger of the experiment due to their capability to provide time measurement.
- A Ionization Hodoscope (IH) detector made up of four layers of scintillator material. This device is able to discriminate double ionization signals expected from pion pairs hitting the same detector element.

The dipole magnet (1.6 T) bends the positive particles in the horizontal plane to the left arm and the negative particles to the right arm. The two spectrometer arms downstream the magnet are composed by a set of identical detectors:

- Four stations of drift chambers (DC1–DC4), making a total of 14 planes, for particle tracking. The single hit resolution is better than 100 μm.
- A plane of Vertical Hodoscopes (VH), and another of Horizontal Hodoscopes (HH). They provide time of flight measurements for triggering purposes.
- A threshold N_2–gas Cherenkov counter (C) used to suppress e^+e^- background pairs.
- A Preshower detector (Psh) made up of Pb plates of several radiation lengths followed by scintillation counters. It is used to improve the electron rejection power and in the trigger system.
- A Muon Detector (MU) to identify muons, located after an iron absorber. It is made up of scintillator slabs.

3.1. The DIRAC multi–level trigger.

Due to the low atomic formation rate ($\sim 10^{-9}$) and the high background, DIRAC needs an efficient multi–level trigger. We trigger simultaneously on time–correlated (real) pairs and time–uncorrelated (accidental) pairs within a time window of $\Delta t = \pm 20$ ns. Several trigger levels are implemented and are discussed in detail in [17], the most relevant are:

- The first trigger level, T1, requires a fast coincidence between detectors in the downstream arms.
- A neural network algorithm, DNA+RNA, is used to select events with with $Q_x < 3$ MeV/c, $Q_y < 10$ MeV/c and $Q_L < 30$ MeV/c. It uses information from the VH, IH, Psh and SFD detectors.
- The last level is composed of a track–finder and analyser using the hit pattern in the drift chambers (DC) to select particle pairs with $Q_L < 30$ MeV/c, $Q_x < 3$ MeV/c.

Triggers on e^+e^+ pairs, lambda decays $\Lambda \to p\pi^-$, and kaon decays $K^\pm \to \pi^+\pi^-\pi^\pm$, are also used for calibration purposes.

4. Method of lifetime measurement.

To obtain the pionium lifetime we need first to measure the breakup probability, $P_{\rm br} = n_A/N_A$, as the ratio of the number of atomic pairs over the number of atoms produced in the target. The DIRAC trigger system collects $\pi^+\pi^-$ pairs in a time window of $\Delta t = \pm 20$ ns (see figure 2), because the method of lifetime measurement requires both accidental (pions coming from different proton interactions in the target) and real pairs. The relative momentum distribution for real (time–correlated) pairs is the sum of three contributions:

$$\frac{dN^{\rm real}}{dQ} = \frac{dN_{NC}}{dQ} + \frac{dN_C}{dQ} + \frac{dn_A}{dQ} \tag{4.1}$$

Where N_{NC} is the number of non–Coulomb pairs, that is, pions coming from long–lived sources and therefore negligible Coulomb interaction between them. N_C is the number of Coulomb pairs coming from short–lived sources. The relative momentum distribution for accidental pairs and for non–Coulomb pairs is the same, because the later are not correlated in relative momentum, but in time. If we denote $dN^{\rm acc}/dQ = dN_{NC}/dQ = \Phi(Q)$, we can write the Coulomb–pairs relative momentum distribution as follows [18]:

$$\frac{dN_C}{dQ} = \Phi(Q)\,(1 + kQ)\,A_C(Q) \tag{4.2}$$

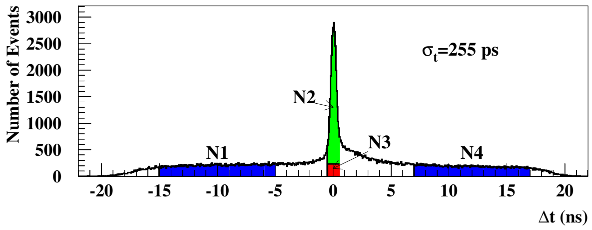

Fig. 2. Time difference spectrum for $\pi^+\pi^-$ pairs.

where the terms $(1+kQ)$ and $A_C(Q)$ take into account strong and Coulomb final state interaction respectively [19]. $A_C(Q)$ is the Coulomb correlation function and it is theoretically known with a precision of about 0.5% [20].

Atomic pairs have a relative momentum $Q < 3$ MeV/c, therefore the distribution of real pairs with $Q > 3$ MeV/c can be described has only two contributions:

$$\frac{dN^{\mathrm{real}}(Q>3)}{dQ} = \frac{dN_{NC}}{dQ} + \frac{dN_C}{dQ} = N\,\Phi(Q)\;[(1+kQ)A_C(Q)+f] \quad (4.3)$$

N, f and k are free parameters to be fitted and $\Phi(Q)$ is measured from accidentals. The number of atomic pairs with $Q < 2$ MeV/c is obtained as an excess of entries in the N^{real} distribution measured in the interval $0 \le Q \le 2$ MeV/c over the prediction from equation (4.3). The number of Coulomb pairs in this interval can also be obtained from equation (4.2) and the best fit parameters.

Since the strong part in the production of $A_{2\pi}$ atoms and Coulomb pairs is the same, the ratio $n_A/N_C = K$ can be computed from (2.1) in a model independent way [14], giving $K = 0.62 \pm 0.01$ for $Q < 2$ MeV/c. In this manner we get the number of atoms produced in the target, $N_A = K\,N_C$, and therefore the breakup probability $P_{\mathrm{br}} = n_A/N_A$. The $A_{2\pi}$ lifetime is extracted comparing this experimental value with the theoretical one, as illustrated in figure 3.

5. Preliminary analysis results.

Here we present the preliminary analysis results of the data taken during the years 2000 and 2001. A small amount of data was also collected in 1999

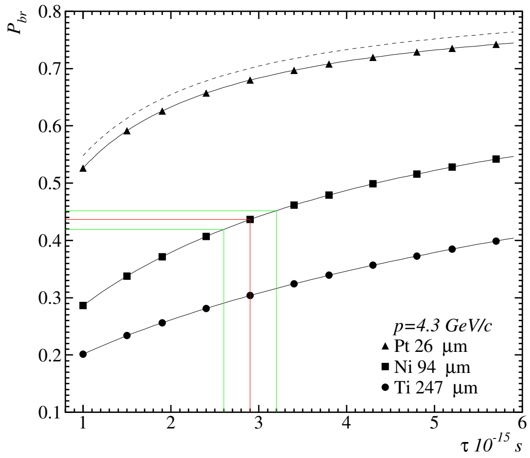

Fig. 3. Theoretical curve showing the $A_{2\pi}$ breakup probability as a function of its lifetime for various targets. The experimental measured breakup probability translates directly into a prediction of the $A_{2\pi}$ lifetime.

at the initial stage of the experiment as a first attempt to observe atomic pairs, but no measurement of the $A_{2\pi}$ lifetime can be extracted from it.

The DIRAC setup delivers a resolution of $\sigma_{Q_L} = 0.57$ MeV/c on the longitudinal component of the relative momentum, and $\sigma_{Q_x} = \sigma_{Q_x} = 0.45$ MeV/c in the transversal components. Rather than working with Q–distributions we define a new variable F, which proves to deliver a better signal to background ratio:

$$F = \sqrt{\left(\frac{Q_L}{\sigma^A_{Q_L}}\right)^2 + \left(\frac{Q_x}{\sigma_{Q_x}}\right)^2 + \left(\frac{Q_y}{\sigma_{Q_y}}\right)^2} \tag{5.1}$$

where $\sigma^A_{Q_L} = 0.65$ MeV/c and takes into account the Q_L–distribution of atomic pairs after ionization. In figure 4 we can see, for example, the F–distribution of accidental, real and atomic pairs for the data taken with a Nickel target during 2000. The atomic pairs are clearly visible at small F. In the following table we summarize the number of atomic pairs found in the analysis of Pt–1999 data, Ni–2000–2001(70%) data and Ti–2000–2001 data.

Target	Z	L(μm)	Atomic pairs ($F < 2$)
Pt	78	28	150 ± 35
Ni	28	94	3590 ± 210
Ti	22	251	1830 ± 160

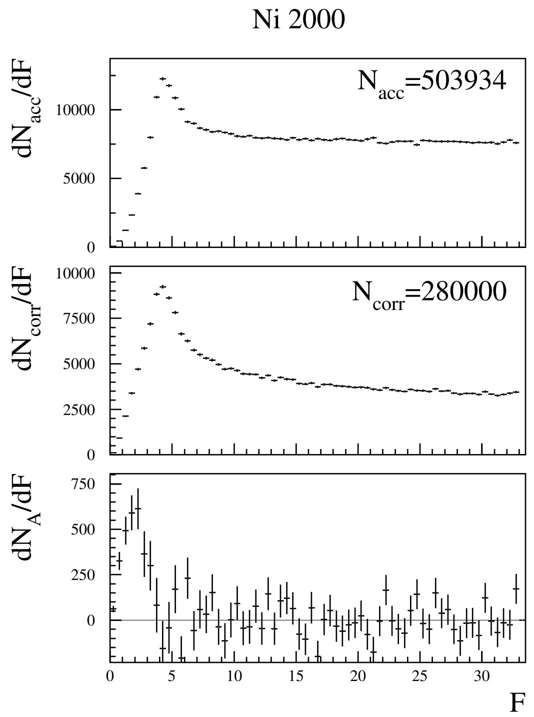

Fig. 4. Distributions on the F variable for accidental pairs (top), time–correlated pairs (middle), and atomic pairs (bottom). N_A in this figure corresponds to n_A in the text.

In the following table we show a preliminary estimation of the statistical sensitivity in our determination of the $A_{2\pi}$ lifetime.

Data sample	Stat. error on $\tau(A_{2\pi})$
Ni (2000)	$\pm 34\%$
Ti (2000/01)	$\pm 26\%$
Ni+Ti	$\pm 22\%$

6. Conclusions.

The DIRAC collaboration has built a fully operational double–arm spectrometer able to deliver a resolution of about 1 MeV/c in the measurement of very low relative momentum particle pairs. We have started to take data in 1999 and have collected around 6000 $\pi^+\pi^-$ pairs from $A_{2\pi}$ atoms breakup. After the analysis of all 2000/01 data, the statistical error will be about 20%. The full statistics, including 2002 data, will allow us to obtain an accuracy of 15% on the lifetime measurement. Further data taking in 2003 is desirable to increase missing statistics and to perform a complete study of systematical uncertainties.

REFERENCES

[1] J. Gasser and H. Leutwyler, Ann Phys. **158** (1984) 142; Nucl. Phys. **B250** (1985) 465.

[2] G. Colangelo, J. Gasser and H. Leutwyler, Nucl. Phys. **B603** (2001) 125.

[3] G. Colangelo, J. Gasser and H. Leutwyler, Phys. Rev. Lett. 86 (2001) 5008.

[4] M. Knecht et al., Nucl. Phys. **B457** (1995) 513.

[5] Nemenov L.L., Yad. Fid. **41** (1985) 980.

[6] L.G. Afanasyev et al., Phys. Lett. **B308** (1993) 200; Phys. Lett. **B338** (1994) 478.

[7] H. Jallouli and H. Sazdjian, Phys. Rev. **D58** (1998) 014011; Erratum: ibid, **D58** (1998) 099901.

[8] M.A. Ivanov et al., Phys. Rev. **D58** (1998) 094024.

[9] J. Gasser, V.E. Lyubovitskij and A. Rusetsky, Phys. Lett. **B471** (1999) 244.

[10] L.G. Afanasyev and A.V. Tarasov, Yad. Fiz. **59** (1996) 2212; Phys. At. Nucl. **59** (1996) 2130. L.G. Afanasyev et al., Jour. Phys. G25 (1999) B7.

[11] Z. Halabuka et al., Nucl. Phys. **B544** (1999) 86.

[12] T.A. Heim et al., J. Phys. B: At. Mol. Opt. Phys. 34 (2001) 3763.

[13] C. Santamarina, Phd. thesis, University of Santiago de Compostela, 2001.

[14] L.G. Afanasyev and O. Voskresenskaya, Phys. Lett. **B453** (1999)

[15] J. Gasser et al., Phys. Rev. **D64** (2001) 016008.

[16] B. Adeva et al., CERN/SPSLC 95-1, SPSLC/P 284. DIRAC Proposal to the SPSLC. CERN/SPSC 2000–032.

[17] L.G. Afanasyev et al., Nucl. Inst. and Meth. **A479** (2002) 407–411. Dubna preprint JINR-E1-2002-32, Feb 2002. 21pp., accepted for publication in NIM.

[18] L.G. Afanasyev et al., Sov. J. Nucl. Phys. **52** (1990) 666; Phys. Lett. **B255** (1991) 146; Phys. of At. Nucl. **60** (1997) 938.

[19] A.D. Sakharov, Zh. Eksp. Teor. Fiz. **18** (1948) 631.

[20] V.N. Bayer and V.S. Fadin, Zh. Eksp. Teor. Fiz. **57** (1969) 225; Sov. Phys. JETP **30** (1970) 120.